Measuring Mitotic Spindle and Microtubule Dynamics in Marine Embryos and Non-model Organisms

Janet Chenevert, Morgane L V Robert, Jérémy Sallé, Sébastien Cacchia, Thierry Lorca, Anna Castro, Alex Mcdougall, Nicolas Minc, Stefania Castagnetti, Julien Dumont, et al.

Measuring mitotic spindle and microtubule dynamics in marine embryos and non-model organisms.

Running Head

Microtubule and spindle dynamics in non-model organisms.

Authors:

Janet Chenevert[1], Morgane L.V. Robert[2,3], Jérémy Sallé[4,5], Sébastien Cacchia[2,3], Thierry Lorca[2,3], Anna Castro[2,3], Alex McDougall[1], Nicolas Minc[4,5], Stefania Castagnetti[1], Julien Dumont[4] and Benjamin Lacroix[2,3*]

1 Sorbonne Universités, CNRS, Laboratoire de Biologie du Développement de Villefranche-sur-mer (LBDV), 06234 Villefranche-sur-mer, France;

2 Université de Montpellier, Centre de Recherche en Biologie cellulaire de Montpellier (CRBM), CNRS UMR 5237, 1919 Route de Mende, 34293 Montpellier cedex 5, France.

3 Programme équipes Labellisées Ligue Contre le Cancer

4 CNRS, Institut Jacques Monod, Université Paris Cité, F-75006 Paris, France

5 Equipe Labellisée LIGUE Contre le Cancer

**correspondance to benjamin.lacroix@crbm.cnrs.fr*

Abstract

During eukaryotic cell division a microtubule-based structure, the mitotic spindle, aligns and segregates chromosomes between daughter cells. Understanding how this cellular structure is assembled and coordinated in space and in time requires measuring microtubule dynamics and visualizing spindle assembly with high temporal and spatial resolution. Visualization is often achieved by the introduction and the detection of molecular probes and fluorescence microscopy. Microtubules and mitotic spindles are highly conserved across eukaryotes, however several technical limitations have restricted these investigations to only a few species. The ability to monitor microtubule and chromosome choreography in a wide range of species is fundamental to reveal conserved mechanisms or unravel unconventional strategies that certain forms of life have developed to ensure faithful partitioning of chromosomes during cell division. Here we describe a technique based on injection of purified proteins that enables the visualization of microtubules and chromosomes with high contrast in several divergent marine embryos. We also provide analysis methods and tools to extract microtubule dynamics and monitor spindle assembly. These techniques can be adapted to a wide variety of species in order to measure microtubule dynamics and spindle assembly kinetics when genetic tools are not available or in parallel to the development of such techniques in non-model organisms.

Key Words

mitotic spindle, microtubule dynamics, non-model organisms, marine embryos, tubulin labeling, histone purification, confocal live imaging.

1. Introduction

Mitotic spindles are self-organized macromolecular structures that partition chromosomes during cell division. At mitotic entry, the interphasic microtubule network is disassembled and reorganizes around the nucleus in radial arrays called asters made of short and highly dynamic microtubules. In most species and cell types, the asters are nucleated around two centrosomes which duplicate during interphase and contribute to the nucleation of a great portion of spindle microtubules. In the early phase of mitosis (prophase), the two microtubule asters contribute to the separation of the centrosomes that migrate to opposite sides of the nucleus and provide bipolarity to the mitotic structure. Following nuclear envelope breakdown (NEBD) microtubules grow towards condensed mitotic chromosomes, align them on a metaphasic plate, then segregate the two sets of chromosomes between the two daughter cells. Numerous microtubule-associated proteins including molecular motors are involved in aster movement, chromosome capture, alignment and segregation, but microtubules and their dynamic properties play a central role in these processes. Indeed, the assembly of the mitotic spindle relies on the dynamic properties of microtubule filaments, hollow cylindrical tubes composed of polymerized alpha-/beta-tubulin heterodimers. This assembly is reversible such that, both *in vivo* and *in vitro*, microtubules stochastically oscillate between phases of growth and shrinkage in a process called dynamic instability [1]. Phases of growth and shrinkage are interspersed with transition events known as catastrophe and rescue. A catastrophe corresponds to a rapid depolymerization event occurring after a growth excursion while rescue corresponds to a regrowth event interrupting a depolymerization phase. The characterization of microtubule dynamics requires the measurement of growth and shrinkage velocities, also called polymerization and depolymerization rates, and of the

frequencies of catastrophe and rescue [2–4]. These four parameters define the dynamic status of individual microtubules but can also be used to predict average microtubule length or collective behavior of microtubule networks and microtubule-based structures [5].

Mitotic spindles and microtubule components are remarkably conserved across eukaryotes. However, depending on cell types or species, the mitotic spindle exhibits high variability of sizes, different nucleation pathways and kinetics of assembly. Despite the variety of forms of life, studies of spindle assembly mechanisms have focused on very few model organisms. This is mostly due to technical limitations because visualizing microtubule dynamics and spindle assembly requires high spatial and temporal resolution, live imaging, and the use of bright fluorescent probes. In genetically tractable organisms, such conditions are met by the use of transgenic strains or cell lines stably expressing fluorescently-tagged proteins to visualize microtubules (tubulins or microtubule binding proteins) and chromatins (histones). Exploring microtubule and mitotic spindle assembly in various species is necessary to understand how distinct and divergent paths could have emerged throughout evolution while resulting in the same outcome. Conversely, identifying conserved mechanisms among a large variety of species will likely reveal the most essential pathways. To apprehend the diversity of microtubule and spindle assembly dynamics we need standardized tools and approaches to enable microtubules and spindle visualization in species even in the absence of genetic tools. Prior to the development of genetic tools and gene editing strategies, in the 1980's, visualization of cellular processes in live cells and embryos was performed using micro-injection of chemically-labeled proteins [6–10]. These approaches have been remarkably useful to reveal the dynamic nature of microtubules and spindles *in vivo* during cell division and to document cell lineage and fate mapping during embryogenesis. However poor

resolution, fluorescent background due to out-of-focus light, and high phototoxicity of light sources were major limitations to the application of this methodology. Today, with the enormous advance in confocal microscopy and high-resolution live imaging, this approach can be adapted to overcome the lack of genetic tools or the inability of some species to translate injected mRNAs during the early stages of embryonic development.

Here we describe an updated protocol for analyzing microtubule dynamics based on protein purification and injection in marine embryos. We present the use of purified and chemically-labeled tubulin and affinity purification of recombinant fluorescent histone coupled to high resolution imaging to follow cell division, monitor mitotic spindle assembly and quantify microtubule dynamics. We also provide standardized methodology for extraction and interpretation of microtubule dynamics parameters as well as an estimation of mitotic spindle assembly kinetics. We are confident that these techniques could be used in a wide variety of species provided that their eggs are transparent enough to be compatible with light microscopy and that they can withstand micro-injection.

2. Materials

2.1. Tissues for tubulin extraction

Visualization of microtubules and spindles in embryos by fluorescence microscopy is facilitated by the injection of "home-made" fluorescent tubulin. The tubulin used for the methodology described here is prepared from freshly collected pig brains (see Notes 1 and 2). Purification and labeling of tubulin are performed as previously described by Castoldi and Popov, and Hyman A.A. [11, 12] and requires the following materials:

1. Fresh brain tissues, preferentially pig brains (see Note 2) collected from a slaughterhouse. Time between slaughtering of the animal, brain collection and protein extraction should be minimized (less than 2 hours) to increase purification yield.
2. Cooler filled with ice and plastic food bags to reduce air and avoid direct contact with ice.

2.2. Tubulin purification and labelling

1. A robust blender to crush brain tissues while avoiding heating.
2. Gauze swabs (not necessarily sterile).
3. Glass Dounce or Potter-Elvehjem homogenizers with glass or PTFE pestle of different volumes. Typically, 50 mL for the first steps, 10 mL and 2 mL for the last steps of tubulin labelling.
4. Refrigerated ultracentrifuge with corresponding tubes for large volumes (250 – 500 mL) with a centrifugal force of at least 25,000 x g.
5. Ultracentrifuge for volumes between 50 to 100 mL and micro-ultracentrifuge with volume < 1 mL able to reach a centrifugal force of at least 50,000 x g for sedimentation of polymerized microtubules. To maximize purification yield, it is recommended to have both warm and cold ultracentrifuges with their respective rotors to minimize time for warming or cooling down of rotors.
6. N-hydroxysuccinimide (NHS) ester fluorescent dye (see Note 3). 5 mg are required to label 50 to 100 mg of tubulin. We usually use 5 mg of N-hydroxysuccinimide (NHS) ester fluorescent dye to label 80 mg of tubulin.
7. Prior to use, NHS dyes are diluted to 50 mM in water-free DMSO.

8. DB (Depolymerization Buffer): 50 mM MES pH 6.6 with KOH, 1 mM $CaCl_2$ (kept at 4°C)
9. Glycerol 100%, kept warm (from hereafter warm means 37°C)
10. HMPB (High Molarity PIPES Buffer): 1 M PIPES pH 6.8 with KOH, 10 mM $MgCl_2$, 20 mM EGTA, kept at 37°C.
11. 5xBRB: 400 mM PIPES pH 6.8 (KOH), 5 mM $MgCl_2$, 5 mM EGTA.
12. 1xBRB (Brinkley BR buffer 80 or BRB80): 80 mM PIPES pH 6.8 with KOH, 1 mM $MgCl_2$, 1 mM EGTA, kept at 4°C. 1xBRB is freshly prepared by diluting 5xBRB with pure water.
13. 150 mM ATP solution. It is recommended to adjust the pH of the solution to pH ~7 using pH paper strips. ATP can be resuspended in 5-10 mM HEPES and then buffered with KOH. Aliquots can be stored at -20 °C.
14. 100 or 200 mM GTP solution. The solution can be adjusted to pH ~7 similarly to the ATP solution. Aliquots can be stored at -20 °C or -80 °C.
15. High pH Cushion: 0.1 M HEPES pH 8.6 (NaOH), 1 mM $MgCl_2$, 1 mM EGTA, 60 % (volume/volume) glycerol.
16. Low pH Cushion: 60 % (v/v) glycerol in 1xBRB.
17. Labeling Buffer: 0.1 M HEPES pH 8.6 (NaOH), 1 mM $MgCl_2$, 1 mM EGTA, 40 % (v/v) glycerol.
18. GDB (Glutamate Depolymerization Buffer): 50 mM Glutamate pH 7.0 (KOH), 0.5 mM $MgCl_2$.
19. 1 M $MgCl_2$ solution in pure water.
20. Centrifuge tubes compatible with DMSO (see Note 4).
21. Ultracentrifuge must be able to function at 4 °C and at 30-37 °C for tubulin polymerization-depolymerization cycles.

2.3. Purification of RFP-histone

1. 1 M solution of IPTG (isopropyl **β**-D-1-thiogalactopyranosid) in water. Store aliquots at -20 °C.
2. BL21(DE3) *E. coli* competent cells.
3. Plasmid pET11-mouseH2B-RFP-6His. Mouse H2B-RFP sequence was obtained from a pCS2 plasmid [13] and subcloned into a pET11 vector for bacterial expression. This plasmid can be provided upon request.
4. LB liquid medium (Luria-Bertani broth). Combine 10 g of tryptone, 5 g of yeast extract, 10 g of NaCl for 1 liter of distilled water; adjust pH to 7.0 with 1 N NaOH and autoclave the mixture for 25 min at 120°C.
5. Ampicillin stock solution at 100 mg/mL in water, stored at -20°C.
6. Lysozyme solution 100x: 10 mg/mL in water.
7. Ultrasonicator with appropriate probe.
8. Refrigerated ultracentrifuge and tubes for at least 30,000 x g.
9. TALON Super flow metal resin or any resin coupled to metal for 6xHistine affinity purification.
10. Empty gravity flow columns.
11. Lysis Buffer: 1x PBS (137 mM NaCl, 2.7 mM KCl, 10 mM Na_2HPO_4, and 1.8 mM KH_2PO_4 supplemented with 300 mM NaCl and protease inhibitors.
12. Buffer A1: 50 mM Tris-HCl pH8, 500 mM NaCl, 5 % Glycerol, 6 M Urea. Store at 4 °C.
13. Buffer A2: 50 mM Tris-HCl pH8, 1M NaCl, 5 % Glycerol, 6 M Urea. Store at 4 °C.
14. Elution buffer: 50 mM Tris-HCl pH8, 500 mM NaCl, 5 % Glycerol, 6 M Urea, 20 mM Imidazole. Store at 4 °C.

15. Dialysis buffer D1: 50 mM Tris-HCl pH 8, 10 mM DTT, 2 mM EDTA, 6 M Urea, 2 M NaCl. Store at 4 °C.
16. Dialysis buffer D2: 20 mM Tris-HCl pH 8, 5 mM DTT, 1 mM EDTA, 1 mM PMSF, 5 % Glycerol, 2 M NaCl. Store at 4 °C.
17. Dialysis buffer D3: 20 mM Tris-HCl pH 8, 5 mM DTT, 1 mM EDTA, 1 mM PMSF, 5 % Glycerol, 1 M NaCl. Store at 4 °C.
18. Dialysis buffer D4: 20 mM Tris-HCl pH 8, 5 mM DTT, 1 mM EDTA, 1 mM PMSF, 5 % Glycerol, 0,5 M NaCl. Store at 4 °C.
19. Dialysis buffer D5: 20 mM Tris-HCl pH 8, 5 mM DTT, 1 mM EDTA, 1 mM PMSF, 5 % Glycerol, 140 mM NaCl. Store at 4 °C.
20. Dialysis tubing, cassette or device compatible with proteins and with a cut-off < 30 kDa.

2.4. Collection or ordering of marine animals

Animal availability varies throughout the year depending on reproductive seasons and on geographical localization (see Note 5). In Europe, wild animal sampling is often not allowed without specific authorities' approval. However, a large variety of species can be obtained from the European Biological Resources Center (EMBRC https://www.embrc.eu and its national branches such as https://www.embrc-france.fr/fr). These infrastructures provide animals while ensuring a regular survey on wild populations limiting the impact of research on ecosystems. Worldwide, researchers can certainly have access to local marine biological resource suppliers. We have successfully used this method in two echinoderm species: the sea urchin *Paracentrotus lividus* [14] and the starfish *Hacelia attenuata*, in a cnidarian the

jellyfish *Clytia hemisphaerica* and a tunicate the ascidian *Phallusia mammillata*. We hope that having tested this methodology in several animals from different and distant taxa provides sufficient evidence that it can be applied to a large variety of species.

2.5. Embryo mounting for injection and imaging.

This chapter aims at the visualization of microtubules and chromatin and the quantification of microtubule dynamics in a wide variety of species. Our methods do not depend on the specific injection procedure, which varies with the species and is highly user dependent. However, we find that a modification of the horizontal injection configuration described previously [15] represents a versatile set-up which is compatible with many types of eggs. We describe here the materials required to build an injection chamber and an imaging chamber for eggs of different sizes.

1. Plastic or metallic customized chamber holder (Figure 1 A and B), (see Note 6)
2. Glass-cutting diamond pen.
3. Artificial or natural filtered sea water.
4. Glass-bottom dishes of 35 mm diameter.
5. Dow Corning high vacuum grease.
6. 10 mL syringe filled with Dow Corning high vacuum grease fitted with a cut-off plastic pipette tip.
7. 22 x 22 mm cover glass.
8. VaLaB: lipid mixture composed of vaseline, lanolin and beeswax at equal 1:1:1 weight proportion.
9. Heating plate which heats to at least 50°C.

2.6. High resolution microscopes

To allow tracking of individual microtubules by fluorescent microscopy, movies must be acquired with an inverted confocal microscope, which provides sufficient temporal and spatial resolution.

1. We have obtained similar image quality and outcomes with spinning disk [14] or swept-field confocal microscopes [16, 17]. Similar images can be achieved with new generation scanning confocal microscopes, especially if equipped with photomultiplier tube of greater quantum efficiency such as gallium arsenide phosphide (GaAsP) PMT or hybrid detector HyD.
2. Objectives should have relatively high numerical apertures (above 1.1) and should allow sufficient imaging depth especially for large embryos. 30x to 60x magnification water or silicon immersion objectives are particularly appropriate for such imaging (see Note 7).
3. Acquisition devices (camera or PMT) must allow a temporal resolution of less than 1 sec.
4. A temperature controller or air conditioning in the microscopy room can be required to maintain temperature compatible with the organism during imaging (see Note 8).

2.7. Image analysis.

1. Data are extracted using the ImageJ software https://imagej.nih.gov/ij/download.html
2. Macros to create kymographs can be downloaded on: https://github.com/benlacroix/ImageJ_Macros

3. Datasheet to extract dynamics data can be found on https://github.com/benlacroix/MTDynamX_Data_Xtraction

3. Methods.

3.1. Purification of tubulin.

Tubulin is purified following a protocol described by Castoldi and Popov [11] based on temperature-induced cycles of polymerization and depolymerization, and the use of a high molarity buffer to remove microtubule associated proteins.

1. Fresh brains obtained at the slaughterhouse should be kept on ice during transport
2. Back at the lab and in a cold room: peel the exterior membranes off of the brains, remove blood vessels and residual pieces of bones and cartilage.
3. Weigh brains and add 1 liter of DB per 1 kg of brain (keep some DB to wash the blender in next steps)
4. Blend 30 seconds at low speed, 30 seconds pause to cool down samples and then 30 seconds at high speed.
5. Filter through double layer of gauze.
6. Centrifuge at 29,000 x g at 4 °C for 1h.
7. Filter the supernatant through the gauze directly from the tubes into a graduated cylinder.
8. Measure volume. This corresponds to the "initial volume" that we will refer to for further steps of this protocol.

9. Add 1 volume of warm HMPB (37 °C) and 1 volume of warm (37 °C) glycerol and mix by inverting.
10. Add ATP to 1.5 mM and GTP to 0.5 mM final concentrations.
11. Mix by inverting and transfer to pre-warmed (37 °C) ultracentrifuge tubes.
12. Incubate 1h at 37 °C preferably in the rotor inside the ultracentrifuge. If the volume exceeds that of your centrifuging capacities, keep the remaining volume in a cylinder at 37 °C in a water bath and repeat the following centrifugation step once the first batch has been pelleted. (Gently manipulate this microtubule solution when transferring in tubes).
13. Pellet polymerized microtubules at 100,000 x g for 30 min at 37 °C.
14. Discard supernatant and resuspend pellet (polymerized microtubules) in a smaller volume of ice-cold DB. Typically 10 mL per 70 mL of initial volume.
15. Homogenize with a Dounce/Potter on ice (20 strokes up and down)
16. Incubate 15 min on ice to depolymerize microtubules
17. Spin this suspension at 4 °C, 120,000 x g for 30 min
18. Keep the supernatant and add: 1 volume of warm HMPB, 1 volume of warm glycerol, 1.5 mM ATP (final) and 0.75 mM GTP (final)
19. Incubate 1h at 37 °C (Incubation can be done directly in centrifuge tubes)
20. Sediment polymerized microtubules by centrifugation at 150,000 x g at 37°C for 30 min.
21. Resuspend the pellet in a minimal volume of ice cold 1x BRB. (Use 10 ml for 500-600 mL of initial volume to get highly concentrated tubulin).

22. Homogenize with a Dounce/Potter on ice and incubate 15 min to depolymerize microtubules.
23. Spin at 100,000 x g at 4 °C for 30 min.
24. The supernatant contains pure tubulin.
25. Measure Absorbance at 280 nm of a 1/10 dilution (in 1x BRB) and calculate the protein concentration given an extinction coefficient of tubulin at 280 nm of 115,000 $M^{-1}.cm^{-1}$ and a molecular weight of 110,000 g/mol for tubulin dimers.

    $C_{(mol/L)}$ = dilution factor · A_{280nm} / 115,000

    $C_{(mg/ml)} = C_{(mol/L)} \cdot 110{,}000$
26. Aliquot (1-2 µL) in microtubes and snap freeze in liquid nitrogen.
27. Store at -80°C.
28. Run 10 µg on a 10% acrylamide SDS-PAGE gel and stain with Coomassie blue. A single strong band of around 50 kDa should appear (see Note 9).

3.2. Labelling of tubulin.

Labelling is performed using NHS (N-HydroxySuccinimide) esters coupled dyes that will react with protein amino groups and create a stable covalent bond. The reaction of NHS esters with amines is pH-dependent, because amines need to be deprotonated. The reaction is thus optimal at “high” pH (here pH 8.6). The reaction is then stopped when the pH is lowered to 6.5-6.8 (typical pH for tubulin buffers) as amines get protonated. A subsequent microtubule polymerization/depolymerization cycle selects for tubulin that is still able to polymerize after labeling and removes excess of free labeling dye.

1. Thaw an aliquot of concentrated tubulin as quickly as possible, and place it on ice as soon as it starts melting.
2. For each labeling reaction, prepare 10 mL of 8 mg/mL tubulin in 1x BRB in a 50 mL Falcon tube by diluting the concentrated tubulin stock. Keep on ice.
3. Bring the $MgCl_2$ concentration to 3.5 mM using a 1 M stock solution (remember that 1x BRB already contains 1 mM $MgCl_2$, i.e., add 25 µL of 1 M $MgCl_2$ per 10 mL of tubulin solution). Bring the GTP concentration to 1 mM using a 100 mM stock solution. Store on ice for 5 min.
4. Transfer to 37 °C and add 5 mL of pre-warmed glycerol to promote polymerization (see Note 10).
5. Let polymerize for 40 min at 37 °C.
6. In an ultracentrifugation tube, layer polymerized tubulin onto a 9 ml warm (37 °C) high pH cushion.
7. Pellet microtubules at 150,000 x g for 45 min at 35 °C (see Note 11). The rotor should accelerate and brake slowly, and the balance tube must contain a 30% glycerol solution on a 60% glycerol cushion to balance properly.
8. Aspirate the supernatant above the cushion and discard it. Rinse the supernatant/cushion interface twice with warm labelling buffer to remove unpolymerized tubulin.
9. Remove the cushion and re-suspend the pellet in 1.9 ml of warm labelling buffer using a cut pipette tip with a wide opening (see Note 12). Keep the tubulin warm during resuspension and continue re-suspending (pipetting up and down) until no aggregates are visible (this takes a while).

10. Resuspend the fluorophore in water-free DMSO to make a 50 mM solution (10x).
11. Add the succinimidyl ester-coupled fluorophore (dissolved in DMSO) in two steps. Add a first half to reach a 2.5 mM final concentration, mix by gentle pipetting. This step must be done in a DMSO compatible tube (see Note 4).
12. Incubate 20 min at 37 °C
13. Add the second half of the fluorophore solution to reach a final concentration of 5 mM (see Note 13). Always pipette into the microtubule solution while slowly rotating the tube by hand. Avoid air bubbles.
14. Keep at 37 °C for 20 min (40 min total incubation with fluorophore), and vortex gently every 5 min. Following this step, always keep the sample covered with aluminum foil to protect it from light.
15. In 2 tubes (polyallomer PA) of appropriate volume, layer the labelling reaction onto 1 ml of pre-warmed low pH cushion.
16. Spin at 120,000 x g for 40 min at 35 °C. Accelerate and brake slowly, typically 30-50% of maximal acceleration/deceleration capacity of your ultracentrifuge.
17. Aspirate the supernatant above the cushion and discard it. Rinse the supernatant/cushion interface twice with warm 1x BRB. Remove the cushion, wash the pellet briefly with warm 1x BRB and re-suspend each pellet in 400 µL of ice-cold GDB (glutamate depolymerization buffer). Homogenize on ice using a Dounce homogenizer. Leave for 30 min on ice. Use another 200 µL of cold GDB to wash tubes and the Dounce homogenizer and pool them with the initial 400 µL.
18. Spin the depolymerized tubulin at 200,000 x g for 10 min at 2 °C.

19. Recover the supernatant from the cold spin, add BRB to 1x final concentration using a 5x stock solution, $MgCl_2$ to 4 mM using a 1 M stock, and GTP to 1 mM using a 100 mM stock. Incubate on ice for 3 min.
20. Warm up to 37 °C for 2 min, add 0.5 volume of pure glycerol, mix well.
21. Polymerize at 37 °C for 30 min. In a 2 to 4 mL ultracentrifuge tube, layer the polymerization reaction onto a prewarmed 1 mL low pH cushion and pellet the microtubules at 150,000 x g for 30 min at 37 °C. Accelerate and brake slowly, typically 30% of maximal acceleration and deceleration.
22. Aspirate the supernatant above the cushion and discard it. Rinse the supernatant cushion interface twice with warm 1x BRB. Remove the cushion and briefly rinse the pellet twice with 1 mL warm 1x BRB. Re-suspend the pellet using a cut pipette tip in 0.2 mL of ice cold 1x BRB.
23. Incubate on ice for 20 min.
24. At this step it is helpful to use a small volume glass 2 mL Dounce/Potter to aid in resuspension and increase recovery.
25. Spin the depolymerized tubulin in a microvolume ultracentrifuge at 200,000 to 250,000 x g for 10 min at 2 °C. Recover the supernatant.
26. Quickly estimate the tubulin concentration, ideally adjust to a final concentration of 20 mg/mL with 1x BRB without GTP (see Note 14) and freeze in 1-2 µL aliquots in liquid nitrogen.
27. Store at -70°C or in liquid nitrogen.

3.3. Purification of histone-RFP.

1. Transform BL21(DE3) competent bacteria with the pET11-HumanH2B-RFP-6His vector and select colonies on ampicillin plate.
2. Pick a single colony and grow overnight in LB medium with 100 mg/L ampicillin.
3. Dilute the culture 1/100 in fresh LB containing 100 mg/L ampicillin and leave shaking at 37°C until it reaches 0.4-0.6 optical density at 600 nm.
4. Transfer the culture to 20°C and induce protein expression by adding IPTG to a final concentration of 0.1 mM.
5. Incubate overnight at 20°C under shaking.
6. Sediment the bacteria at 4000 x g for 20 min at 4 °C.
7. Resuspend the bacterial pellet in lysis buffer containing 0.1 mg/mL lysozyme. At this step, the bacterial suspension can be stored at -80°C.
8. Incubate the suspension for 30 min at 4 °C on a rotating wheel.
9. Place the suspension in a 50 mL plastic centrifugation tube in a plastic beaker filled with ice and water. Clean the ultrasonicator probe with water and alcohol. Dip the probe into the tube (3/4 depth). Sonicate at a 40% amplitude, with pulses of 1 sec on/3 sec off, for 1 minute total or until the solution becomes less viscous.
10. Ultracentrifuge at 30,000 x g for 30 min at 4 °C. Insoluble proteins will be found in the pellet. Discard the supernatant.
11. Resuspend the pellet with buffer A1 and homogenize using a Dounce/Potter.
12. Ultracentrifuge at 30,000 x g for 30 min at 4 °C.
13. Collect the supernatant containing the soluble proteins.
14. Centrifuge the TALON Super flow metal resin at 500 x g for 2 min at 4°C and wash it three times with buffer A1.

15. Incubate the resin with the supernatant from step x (13) overnight at 4°C on a rotating wheel.
16. Wash the resin three times with 10 mL of buffer A1.
17. Wash the resin three times with 10 mL buffer A2.
18. Wash once more with buffer A1.
19. Place the resin in a gravity flow column and wash with a solution containing 2% buffer B1 and 98% buffer A1 to remove non-specific proteins.
20. Elute the H2B-RFP His-tagged protein using a small volume of elution buffer, collecting 0.5-1 mL fractions become near colorless.
21. Run proteins on a 10% SDS-polyacrylamide gel and check protein purity by Coomassie staining.
22. Quantify protein concentration using the Bradford assay or equivalent method.
23. Pool the most concentrated fractions containing pure protein and transfer the solution to a dialysis device (tube or cassette).
24. Dialyze the protein with dialysis buffer D1 overnight at 4 °C to remove imidazole.
25. Then dialyze the sample with dialysis buffer D2 for 4 h to overnight at 4 °C to remove urea.
26. Remove aggregates by centrifuging the sample at 30,000 x g for 20 min at 4 °C.
27. Dialyze the supernatant with dialysis buffer D3 for 4 h to overnight at 4 °C.
28. Dialyze with dialysis buffer D4 for 4 h to overnight at 4 °C.
29. Dialyze with dialysis buffer D5 overnight at 4 °C.
30. Centrifuge proteins at 30,000 x g for 20 min at 4 °C to remove aggregates.
31. Make small aliquots (2-4 µL) from the supernatant.

32. Freeze in liquid nitrogen and store at -80°C.

3.4. Assembly of injection chambers.

We use an injection chamber adapted from Jaffe and Terasaki [18] which can be adjusted to embryos of distinct sizes (Figure 1A-C).

1. Using the diamond glass cutter pen, cut small glass pieces (about 5 x 10 mm) from a coverslip. This will serve as the "ledge" against which the eggs will align.
2. With a pipette tip or glass capillary, apply a small amount of VaLaB to one side of the ledge. Place it on a 22 x 22 cover glass, about 2 mm from the edge.
3. Place the coverslip + ledge on a warm heating plate (50 °C) for a few minutes.
4. Remove the coverslip + ledge and let it cool down.
5. If the eggs to be injected are larger than 150 µm diameter, add another overlapping glass piece with VaLaB, so the ledge will be taller than the egg.
6. Take the customized chamber holder and using the Dow Corning grease-filled syringe, apply a thin line of grease to both sides of the U-shaped opening.
7. Attach the glass coverslip + ledge to the chamber holder on the objective side (bottom). Press the grease to seal it flat.
8. Seal a second 22 x 22 mm glass coverslip on the other (top) side of the holder to complete the chamber (Figure 1 A and B).
9. The injection chamber can now be filled with sea water (or other liquid media for live embryos).
10. Pipette the eggs into the injection chamber, near to the open side but at a safe distance from the opening and exposure to air.

11. Tilt the holder slightly so the eggs will line up along the ledge by gravity, then place it on the microscope stage for injection.

3.5. Preparation of proteins for injection

1. Protein aliquots are thawed quickly by holding them in hand or placing them into room temperature water.
2. As soon as liquid appears on tube walls, place the tubes on ice.
3. Tubulin is diluted in calcium-free 1xPBS to a concentration of 2 to 4 mg/mL.
4. H2B-RFP protein is used at a concentration of 4 mg/ml diluted in calcium free 1xPBS.
5. When mixed together, tubulin is diluted directly in the histone solution.
6. To remove aggregates, centrifuge the mixture at 10,000 x g for 5 min at 4°C

3.6. Injection

We recommend trying different dilutions and injection volumes. Injection of a large excess of tubulin can cause premature pole fragmentation in anaphase, formation of cortical arrays in meiotic eggs or during mitosis, asymmetric cleavage or loss of cell cycle synchrony [14].

1. Injected volume is estimated to be between 1 and 10% of the volume of the egg as previously described [8].
2. This volume can be calibrated by measuring the diameter of an aqueous droplet injected into an oil droplet using similar injection parameters. In some eggs we see a transient round clearing in the cytoplasm upon injection which gives a direct estimate of the injected volume.

3.7. Mounting of injected embryos for imaging

1. Place a drop of seawater onto the glass of a glass-bottom dish, 100 to 120 µL for a 35 mm diameter dish (Figure 1D).
2. Pipette the injected and fertilized eggs into the drop.
3. Using a syringe filled with Dow Corning grease, apply a thin outline of grease around but not touching the drop.
4. Place a 22 x 22 mm glass coverslip on top of the drop taking care not to trap air bubbles near the eggs.
5. Press gently on the coverslip to stabilize its contact with the drop and the grease.

3.8. Acquisition settings on confocal microscopes

When mitotic spindles assemble perpendicular to the light path (parallel to the slide), the observer can easily visualize long microtubule trajectories within different subcellular populations of microtubules. In this case, 2D spatial imaging (x-y-t) will be sufficient to observe and track microtubules with high temporal resolution. The key requirement to measure microtubule dynamics, in addition to a high signal-to-noise ratio, is a frame rate between 0.5 and 2 images per second [3, 14, 16]. If microtubules grow at a speed of 0.4 µm/s and the frame rate is 1 image per second, a pixel size of 200 nm would be appropriate, and the objective should be chosen accordingly. This pixel size is typically achieved with 60x oil immersion objectives on most cameras. Water or silicon immersion objectives can also be used with thicker specimens, which is often the case for marine embryos.

3.9. Measurement of microtubule dynamics from movies

1. To better visualize microtubule tracks, create a maximal intensity projection of the time frames corresponding to the period over which you want to extract dynamics parameters (*Image>Stack>Z Project…*), (see Note 15).
2. Microtubule tracks are drawn on the Max Intensity Projections or directly on the stack using the "Segmented line tool" in ImageJ.
3. Every track position is recorded in the Region of Interest Manager (ROI) (*Edit>Selection>Add to Manager*) or by pressing "T" on the keyboard.
4. Select all the tracks and save them as an RoiSet.zip file (*More>Save*). This RoiSet.zip can be renamed and saved with the corresponding image sequence. It can be re-opened anytime to reuse, modify or add any ROI.
5. Kymographs can then be created for each ROI using our macro "*Multi_ROI_kymo.ijm*" (available on https://github.com/benlacroix/ImageJ_Macros). This macro will create a kymograph for each ROI and save them as individual images in a single folder (see Note 16).
6. Kymographs in ImageJ represent the signal in grey value of the ROI (each ROI is a line corresponding to a microtubule track) with the horizontal and vertical axes corresponding to distance and time respectively. Each horizontal pixel corresponds to a distance equal to pixel size in the acquired image and each vertical pixel represents a single frame of the image sequence.
7. Dynamics data is extracted manually on each kymograph by measuring the slope (Straight lines command) of polymerization and depolymerization events (Figure 2A).

To do so, draw a line that matches each event of interest and press the M key (*Analyse>Measure*).

8. ImageJ will open a "Results" window that can be saved as a .csv file and imported in a spreadsheet software. The user can set which measurements are displayed in this window. To extract dynamics parameters the "Angle" and the "Length" of each slope are required.

3.10. Analysis and interpretation of dynamic properties

1. Example files to practice data extraction are available on https://github.com/benlacroix/MTDynamX_Data_Xtraction
2. Angles are measured following a trigonometric circle (counter clockwise) by ImageJ but are displayed in degrees. Slopes of growing microtubules therefore generate an angle in degrees between 0 and -90 degrees. Depolymerization events generate an angle between -90 and -180 degrees and pause events an angle α = -90 or = 90 degrees (see Note 17 and 18).
3. Polymerization (0° > α > -90°) and depolymerization (-90° > α > -180°) can be easily sorted by their angle value.
4. Velocities (distance/time) can be extracted from these measurements as they correspond to the inverse of the tangent of the angle measured by ImageJ (Figure 2A). For this calculation, angles in degrees must be converted into radians.
5. Similarly, growth or shrinkage duration can be extracted using the sine of the angle and the length of the straight line drawn on growth and shrinkage events (see section 3.9). Catastrophe and rescue frequencies are calculated respectively as the inverse of

the average growth duration and the inverse of the average shrinkage duration (see Note 19).

6. Polymerization and depolymerization distances are extracted using cosine of the angle measured by ImageJ and the corresponding length.

3.11. Determining the regime of microtubule dynamics

In mitosis, microtubule catastrophe is high and microtubules depolymerize all the way to the spindle poles [5, 19, 20]. The consequence of this behavior is that the average microtubule length is restricted by the microtubule dynamics properties. This dynamic state corresponds to the "bounded" regime [5] as opposed to the "unbounded" regime of interphasic microtubules, which tend to continuously elongate. Verde et al. proposed a mathematical model and a simple equation that describes the dynamic regime of microtubules using the observed values of the four dynamics parameters (equation #1 Figure 2B, [5]). The value of microtubule average velocity ("J") becomes negative when microtubules are in the bounded regime and positive in the unbounded regime. In addition, in the bounded regime, it is possible to predict the average microtubule population length ($<L>$) using the equation #2 (Figure 2B) proposed by Verde et al. [5]. The mathematical estimation of microtubule average length can be useful if microtubule length cannot be determined experimentally.

3.12. Assessing spindle assembly by measuring spindle length

Spindle assembly can be followed by measuring the distance between spindle poles or between centrosomes throughout spindle assembly and plotting this distance over time.

1. Based on tubulin fluorescence intensity, draw a straight line between the two points at the center of the two asters (Figure 2C).
2. Measure the length of this line (*Analyse>Measure)* and repeat this process for every time point.
3. Plot the measured distances relative to time to follow the evolution of spindle length.

3.13. Assessing spindle assembly by measuring tubulin intensity within the spindle

Depending on the cell type, the distance between asters or centrosomes may not always be a valid readout of spindle assembly because this distance does not necessarily increase. In addition, this distance does not reflect how the mitotic spindle assembles in 3D. A more valuable readout to estimate spindle assembly could therefore be to measure the spindle mass [21, 22] defined by the quantity of microtubules (or tubulin) assembled in the structure. We found that following the evolution of the microtubule density (tubulin signal) within the spindle can serve as a simple and useful proxy to estimate spindle assembly kinetics (Figure 2C).

1. Make sure that the spindle or the embryo does not move or drift during the time of spindle assembly (see Note 20)
2. Select an ROI remaining within the spindle from NEBD through to anaphase.
3. Use the command "Measure Stack" (*Image>Stack>Measure Stack).*
4. Plot the integrated density or the mean gray value over time. As shown in Figure 2C, the intensity will begin to increase at NEBD and will reach a plateau at metaphase.

3.14. Identification of mitotic phases using the histone marker

Injection and imaging of recombinant RFP-histone can be performed to better define the stages of cell division in each species (Figure 3) and compare with the results obtained using tubulin. Mitotic progression is easier to visualize using a chromatin marker as NEBD, metaphase and anaphase onset will be clearly identified (Figure 3C).

1. NEBD can be characterized by following RFP-histone background intensity within nuclear area. At NEBD, this diffuse RFP-histone signal within the nuclear area drops suddenly as proteins become diluted in the cytoplasm.
2. Cells are considered in metaphase when chromosomes are all aligned on a single plate.
3. We define anaphase onset as the first timepoint where a clear separation between sister chromatids is observed.

4. Notes

1. Commercially available fluorescent tubulin can also be used. However, in our hands, some batches gave rise to aggregation and poor signal-to-noise ratio impeding visualization of microtubule fibers.
2. Pig versus bovine tubulin. We recommend the use of pig brain rather than bovine for 2 main reasons. First, we observed that *in vitro* the critical concentration necessary for tubulin polymerization was higher for bovine tubulin. Thus, a higher tubulin concentration is necessary for similar polymerization kinetics. Secondly the term "bovine" at the slaughterhouse refers to any individual of the species *Bos taurus* and

can include animals of very different ages and selected for different purposes (milk, meat, calving, etc.). "Pig" instead refers to *Sus scrofa* of a relatively narrow range of age (between 6 and 9 months) mostly dedicated to meat products. It is mainly to avoid these age differences and variability in protein quality that we prefer pig brain as tubulin source.

3. We used ATTO 488 and ATTO 565 in our experiments as they have a relatively high fluorescence quantum yield and are resistant to photobleaching.
4. Polysuflone, PVC or polycarbonate do not withstand high concentration of DMSO. The labeling reaction can be initiated in polypropylene tubes which are DMSO-compatible. Once DMSO concentration has been diluted (to < 10 %), the solution can be transferred to any type of ultracentrifugation tubes. For tubulin labelling, as the volumes are relatively small, it is recommended to have access to a microvolume (less than 1ml) ultracentrifuge with high-speed capacity (>50,000 x g).
5. The geographical dependence for animal availability is illustrated by the use of sea urchin species, for example *Strongylocentrotus purpuratus* is present on the west coast of North America but absent from the east coast and European shores. We know from our previous work and past studies that injection of tubulin is a valuable tool to study spindle assembly in *Lytechinus variegatus* (East coast of North America) and *Paracentrotus lividus* (European Atlantic and Mediterranean coasts), [8, 10, 14].
6. The custom holder can be adjusted for every injection set-up but typically has the dimensions of a standard microscopy slide (75 x 25 mm). It should have a U-shaped opening, which allows both good visibility with the objective (using an inverted microscope) and access from the side for a pipette or injection needle. The thickness

should not be too high (less than 6 mm) to allow surface tension to maintain sea water in the chamber [15].

7. Egg size can be a limiting factor since the signal will decay with distance from the microscope objective. Higher magnification and numerical aperture objectives usually have shorter working distance. Using water immersion 40x magnification objective with 1.1 numerical aperture, we have imaged specimens as large as 210 µm diameter using *Clytia hemisphaerica* embryos.
8. As microtubule dynamics parameters are temperature sensitive [23, 24] it is advisable to maintain consistency in temperature during and between acquisitions.
9. Depending on the acrylamide quality and on the bis-acrylamide concentration in the SDS-PAGE gel, alpha- and beta-tubulin can potentially be separated and appear as two separate bands.
10. The solution might become turbid very quickly during addition of glycerol. This does not affect polymerization efficiency.
11. Temperature during centrifugation is set at 35 °C to avoid rotor or centrifuge overheating, which would alter protein quality.
12. This is achieved by cutting off around 5 millimeters from the narrow opening of a pipette tip as the pellet may otherwise clog the tip.
13. The molecular ratio for labeling should correspond to a 10 to 20-fold excess of fluorophore molecules per tubulin molecule. We estimate tubulin amount assuming 70% polymerization efficiency and a molecular weight of 110,000 g/mol. Final DMSO concentration should be ≤ 10%.

14. We do not add GTP to the tubulin in order to reduce risk of polymerization in the injection needle. GTP at a concentration of 0.1 mM is usually used for long-term storage of tubulin, however we have injected and imaged labelled tubulin stored without GTP for 8 years at -70°C without any obvious sign of alteration.
15. Although called "Z-project", this is a timeseries so it corresponds here to a temporal projection.
16. In the macro "*Multi_ROI_kymo.ijm*" as in the "MultipleKymograph" plugin, the linewidth on which the kymograph is made can be adjusted. If n > 1, the signal of n pixels will be averaged. Larger linewidths are more likely to capture microtubule events if the fibers move slightly but the resulting kymograph will become blurry. We usually use n = 1 or 3.
17. Microtubule rescue is very rarely detected in mitosis as microtubules usually depolymerize all the way to the organizing center where the tubulin signal is too strong to enable observing such events. Thus, rescue frequency of mitotic microtubules can be considered null [5]. In addition, mathematical modeling of microtubule length in mitosis suggests that the rescue frequency has little impact on microtubule length and behavior and can therefore be neglected [5]. It can therefore seem counter-intuitive to define microtubule rescue as the inverse of the average depolymerization time, which provides a non-null value. However, assessing this parameter can still be relevant since microtubules depolymerize rapidly (high shrinkage rate) and frequently (high catastrophe frequency) maintaining a large pool of soluble tubulin that, together with centrosomal nucleation, ensures that new microtubule growth will compensate for the loss of microtubules.

18. Pause events are very rare in mitosis and were never observed in any of our observations on spindle microtubules.
19. *In vivo*, it can be hard to observe the total life history of individual microtubules. Walker et al. proposed to estimate catastrophe frequency as the inverse of the average time spent growing [2]. Technically, this frequency is assessed by averaging the growth duration of multiple microtubules observed in a given time period.
20. If the object drifts or moves during imaging, several recalibration or "registration" softwares or ImageJ plugins are available to correct for this movement.

Acknowledgments

We thank all members of Alex McDougall's lab and Stefania Castagnetti's lab at LBDV, IMEV in Villefranche-sur-mer, France, Julien Dumont's lab in Institut Jacques Monod in Paris and Anna Castro's and Thierry Lorca's lab at CRBM in Montpellier, France. We are grateful to the Clytia team especially Evelyn Houliston and Tsuyoshi Momose at IMEV for their assistance and for providing *Clytia hemisphearica* gametes. We thank Carsten Janke's lab (Institut Curie, Orsay France) for providing help with tubulin purification and Lydia Besnardeau (LBDV, IMEV) for cloning the pET11-mouseH2B-RFP-6His plasmid. We are also grateful to Christian Sardet for fruitful discussions and his inspiring comments. This work benefited from access to the Institut de la Mer de Villefranche including the Imaging Platform PIM (member of MICA microscopy platform), an EMBRC-France and EMBRC-ERIC Site, Financial support was provided by ANR-10-INBS-02. The project was initiated thanks to EMBRC FR – AAP2019 – n° 3238 (B. Lacroix). The work was funded by ANR MTDiSco ANR-20-CE13-0033 (B. Lacroix) and European Research Council ERC-CoG ChromoSOMe 819179 (J. Dumont).

References

1. Mitchison T, Kirschner M (1984) Dynamic instability of microtubule growth. Nature 312:237–42

2. Walker RA, O'Brien ET, Pryer NK, et al (1988) Dynamic instability of individual microtubules analyzed by video light microscopy: rate constants and transition frequencies. J Cell Biol 107:1437–48

3. Shelden E, Wadsworth P (1993) Observation and quantification of individual microtubule behavior in vivo: microtubule dynamics are cell-type specific. J Cell Biol 120:935–45

4. Zwetsloot AJ, Tut G, Straube A (2018) Measuring microtubule dynamics. Essays Biochem 62:725–735. https://doi.org/10.1042/EBC20180035

5. Verde F, Dogterom M, Stelzer E, et al (1992) Control of microtubule dynamics and length by cyclin A- and cyclin B-dependent kinases in Xenopus egg extracts. J Cell Biol 118:1097–108

6. Minden JS, Agard DA, Sedat JW, Alberts BM (1989) Direct cell lineage analysis in Drosophila melanogaster by time-lapse, three-dimensional optical microscopy of living embryos. J Cell Biol 109:505–516. https://doi.org/10.1083/jcb.109.2.505

7. Kellogg DR, Mitchison TJ, Alberts BM (1988) Behaviour of microtubules and actin filaments in living Drosophila embryos. Development 103:675–686. https://doi.org/10.1242/dev.103.4.675

8. Wadsworth P, Sloboda RD (1983) Microinjection of fluorescent tubulin into dividing sea urchin cells. Journal of Cell Biology 97:1249–1254. https://doi.org/10.1083/jcb.97.4.1249

9. Hamaguchi Y, Toriyama M, Sakai H, Hiramoto Y (1985) Distribution of fluorescently

labeled tubulin injected into sand dollar eggs from fertilization through cleavage. J Cell Biol 100:1262–1272. https://doi.org/10.1083/jcb.100.4.1262

10. Salmon ED, Leslie RJ, Saxton WM, et al (1984) Spindle microtubule dynamics in sea urchin embryos: analysis using a fluorescein-labeled tubulin and measurements of fluorescence redistribution after laser photobleaching. J Cell Biol 99:2165–2174. https://doi.org/10.1083/jcb.99.6.2165

11. Castoldi M, Popov AV (2003) Purification of brain tubulin through two cycles of polymerization-depolymerization in a high-molarity buffer. Protein Expr Purif 32:83–8. https://doi.org/10.1016/S1046-5928(03)00218-3

12. Hyman AA (1991) Preparation of marked microtubules for the assay of the polarity of microtubule-based motors by fluorescence. J Cell Sci Suppl 14:125–7

13. Prodon F, Chenevert J, Hébras C, et al (2010) Dual mechanism controls asymmetric spindle position in ascidian germ cell precursors. Development 137:2011–2021. https://doi.org/10.1242/dev.047845

14. Lacroix B, Letort G, Pitayu L, et al (2018) Microtubule Dynamics Scale with Cell Size to Set Spindle Length and Assembly Timing. Dev Cell 45:496-511 e6. https://doi.org/10.1016/j.devcel.2018.04.022

15. Yasuo H, McDougall A (2018) Practical Guide for Ascidian Microinjection: Phallusia mammillata. Adv Exp Med Biol 1029:15–24. https://doi.org/10.1007/978-981-10-7545-2_3

16. Lacroix B, Bourdages KG, Dorn JF, et al (2014) In situ imaging in C. elegans reveals developmental regulation of microtubule dynamics. Dev Cell 29:203–16. https://doi.org/10.1016/j.devcel.2014.03.007

17. Lacroix B, Maddox AS (2014) Microtubule dynamics followed through cell

differentiation and tissue biogenesis in C. elegans. Worm 3:e967611. https://doi.org/10.4161/21624046.2014.967611

18. Jaffe LA, Terasaki M (2004) Quantitative Microinjection of Oocytes, Eggs, and Embryos. Methods Cell Biol 74:219–242

19. Belmont LD, Hyman AA, Sawin KE, Mitchison TJ (1990) Real-time visualization of cell cycle-dependent changes in microtubule dynamics in cytoplasmic extracts. Cell 62:579–89

20. Verde F, Labbe JC, Doree M, Karsenti E (1990) Regulation of microtubule dynamics by cdc2 protein kinase in cell-free extracts of Xenopus eggs. Nature 343:233–8. https://doi.org/10.1038/343233a0

21. Mitchison TJ, Ishihara K, Nguyen P, Wuhr M (2015) Size Scaling of Microtubule Assemblies in Early Xenopus Embryos. Cold Spring Harb Perspect Biol 7:a019182. https://doi.org/10.1101/cshperspect.a019182

22. Rieckhoff EM, Berndt F, Elsner M, et al (2020) Spindle Scaling Is Governed by Cell Boundary Regulation of Microtubule Nucleation. Current Biology 30:4973-4983.e10. https://doi.org/10.1016/j.cub.2020.10.093

23. Srayko M, Kaya A, Stamford J, Hyman AA (2005) Identification and characterization of factors required for microtubule growth and nucleation in the early C. elegans embryo. Dev Cell 9:223–36. https://doi.org/10.1016/j.devcel.2005.07.003

24. Li G, Moore JK (2020) Microtubule dynamics at low temperature: evidence that tubulin recycling limits assembly. Mol Biol Cell 31:1154–1166. https://doi.org/10.1091/mbc.E19-11-0634

Figure

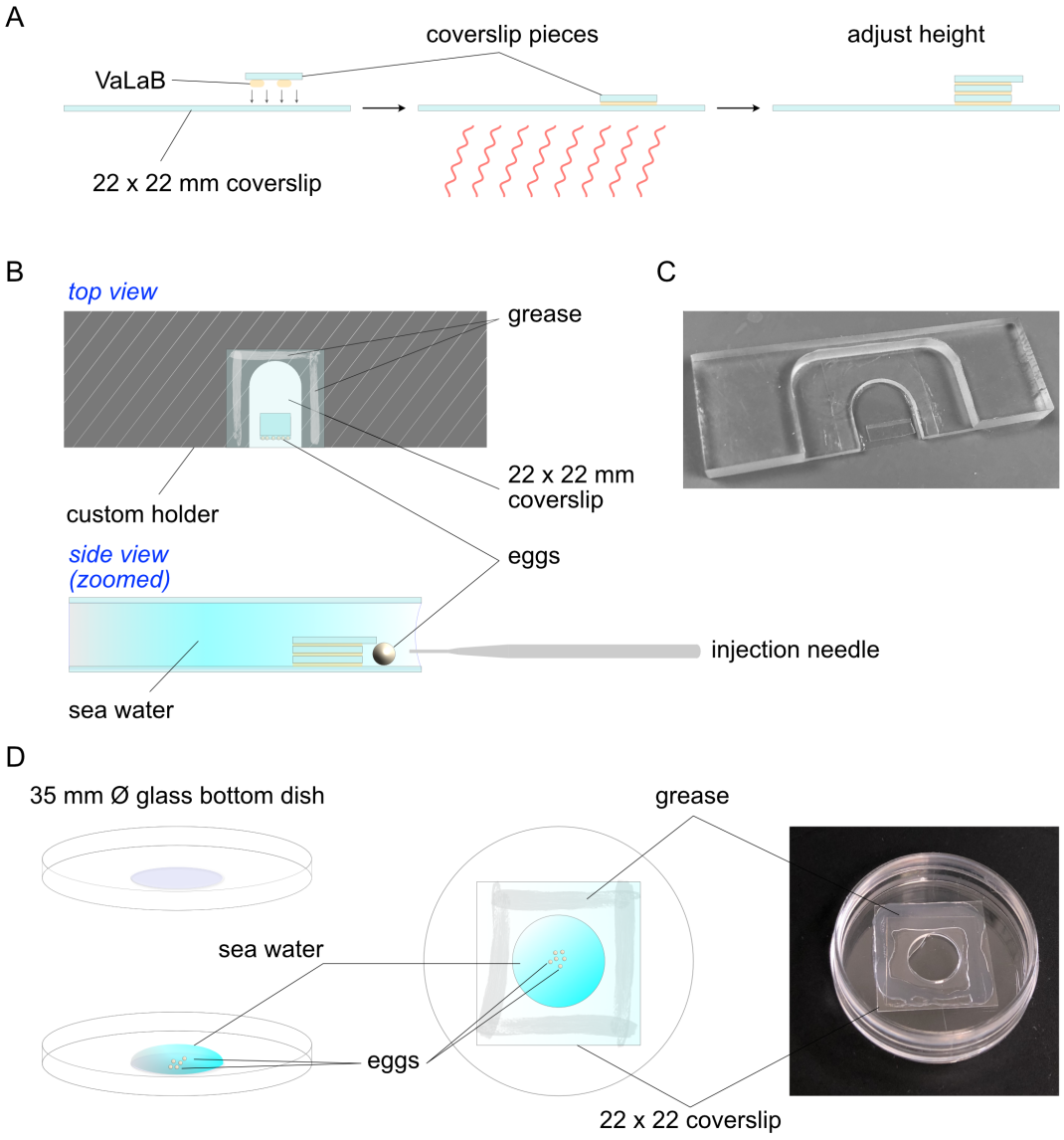
A
coverslip pieces
adjust height
VaLaB
22 x 22 mm coverslip
B
top view
grease
22 x 22 mm coverslip
custom holder
eggs
side view (zoomed)
injection needle
sea water
C
D
35 mm Ø glass bottom dish
grease
sea water
eggs
22 x 22 coverslip

Figure 1. Chambers for injection and live imaging.

(A) Schematic representation (side view) of how to prepare a glass ledge to align eggs for horizontal injection (inspired by Jaffe and Terasaki [18]). Small pieces of glass are stacked and glued with wax (VaLaB) onto a coverslip to create a ledge of the height of the egg to be injected. The wax melts with addition of heat (red wavy lines) and solidifies in place when returned to room temperature. (B) Diagram depicting creation of the injection chamber. Using Dow Corning grease, the coverslip containing the ledge is sealed to the bottom and another coverslip is sealed on top of the U-shaped opening in the plastic holder. Side view shows an egg is immobilized by compression between the ledge and the needle. (C) Picture of an injection chamber. (D) Live imaging chamber used for inverted confocal microscopy. A drop (~100 µL) of sea water is placed on the glass bottom of a 35 mm diameter dish. Fertilized eggs are placed into the sea water drop. The chamber is closed with a 22 x 22 mm coverslip sealed with Dow Corning grease at the edges to avoid evaporation and contact with air. These chambers allow for up to 24 hours of normal development.

A

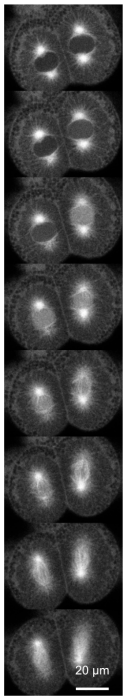

"Segmented line"

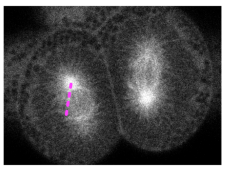

"MultipleKymograph"

"Straight line"

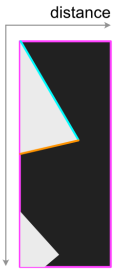

"Measure"

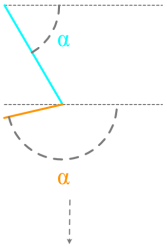

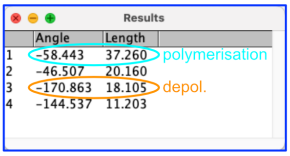

$\alpha_{RAD} = \alpha_{DEG} \cdot \pi/180$ ------ convert degree Angle in radian

$\mathbf{V_g}$: growth velocity = 1 / tan(α_{RAD}) · pixel size · n_{fps}

$\mathbf{f_{cat}}$: catastrophe frequency = 1 / average(time of growth) time of growth = (sinα · Length) / n_{fps}

$\mathbf{V_s}$: shrinkage velocity = 1 / tan(α_{RAD}) · pixel size · n_{fps} time of shrinkage = (sinα · Length) / n_{fps}

$\mathbf{f_{res}}$: rescue frequency = 1 / average(time of shrinkage)

*n_{fps} = number of frame per second

B

equation #1

$$J = \frac{V_g \cdot f_{res} - V_s \cdot f_{cat}}{f_{cat} + f_{res}}$$

equation #2

$$\langle L \rangle = \frac{V_s \cdot V_g}{V_s \cdot f_{cat} - V_g \cdot f_{res}}$$

C

NEBD

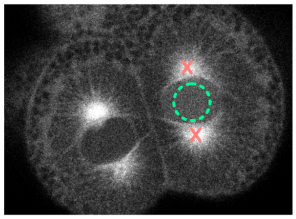

metaphase

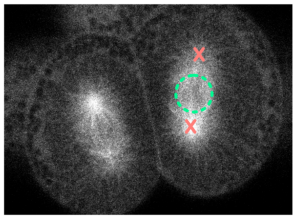

NEBD: Nuclear Envelope BreakDown

AO: Anaphase Onset

Spindle size or mass

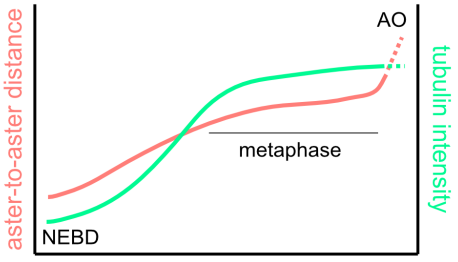

Figure 2. Extraction of microtubule dynamics and spindle assembly properties.

(A) Extraction of microtubule dynamics using kymographs. The images show fluorescent tubulin in two cells entering mitosis, from a timelapse movie of a *P. mammillata* embryo. In quotes are the ImageJ tools and functions used for the analysis. Using "Segmented line" tool, individual microtubule tracks are drawn. Kymographs are then generated from the movies using the plugin "*MultipleKymograph*" (embedded in the macro "*Multi_ROI_kymo.ijm*", see 3.9 step 5.). "Straight line" tool is then used to draw the slopes corresponding to polymerization events (cyan) and depolymerization events (orange). ImageJ can then "Measure" and report the "Angle" and the "Length" for each individual slope. Growing microtubules therefore generate an angle between 0 and -90 degrees (cyan). Depolymerization events generate an angle between -90 and -180 degrees (orange). Angles are converted to radians and each parameter is extracted using the formulas shown. (B) Equation #1 is used to estimate the average growth rate of the entire microtubule population. In mitosis, this should be a negative number (bounded regime) [5]. Equation #2 estimates the average microtubule length (only if microtubules are in the bounded regime). (C) Using time lapse sequences, spindle length can be extracted over time by measuring aster-to-aster distance (red). Alternatively, tubulin intensity within the spindle area can be analyzed overtime to follow spindle assembly (green curve).

A

C. hemisphaerica at 4-cell stage

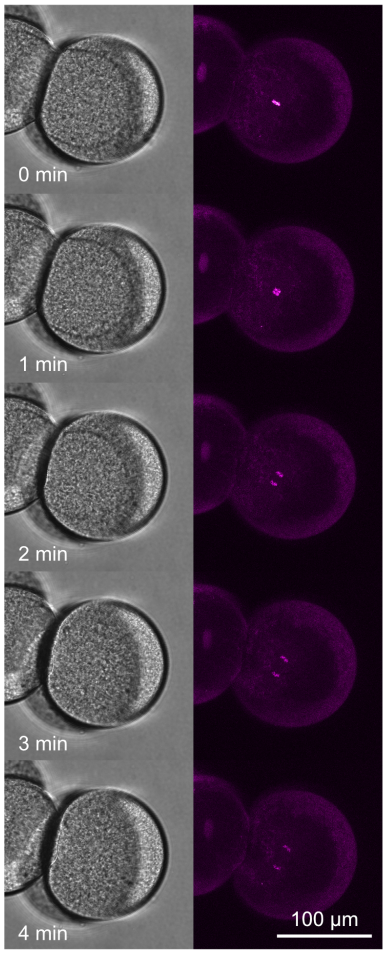

B

P. mammillata at 32-64-cell stage

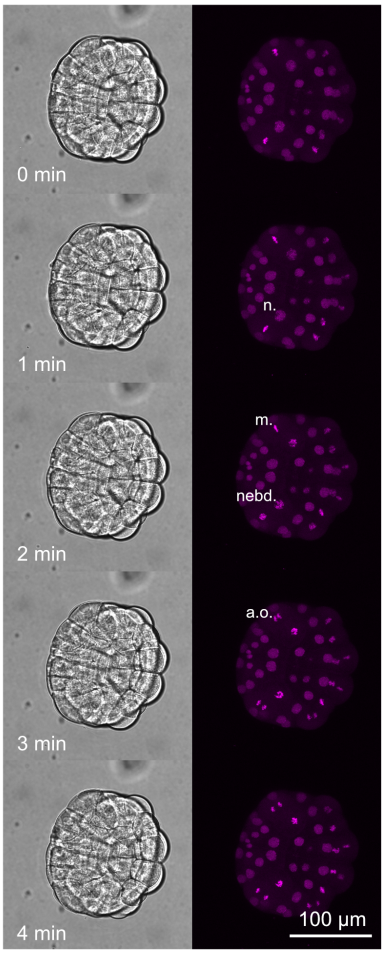

C

nucleus before envelope breakdown

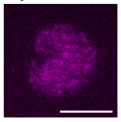

nuclear envelope breakdown

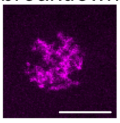

metaphase

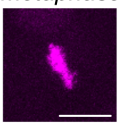

anaphase

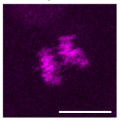

nuclear envelope reformation

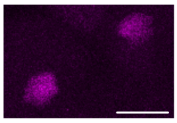

Figure 3. Mitotic landmarks visualized using histone H2B-RFP as chromatin marker.

(A) Images from a time lapse acquisition of a *Clytia hemisphaerica* embryo derived from an egg injected with histone H2B-RFP protein and imaged on a confocal microscope. Transmitted light on the left, RFP emission signal (561 nm) on the right (magenta). (B) Same as (A) for a *Phallusia mammillata* embryo. On the RFP signal (magenta) mitotic events can be observed: n.: nucleus prior to nebd: nuclear envelope breakdown; m.: metaphase plate; a.o.: anaphase onset. (C) Selected images from a timelapse sequence showing DNA (H2B-RFP signal, magenta) in a single cell of a developing *Phallusia mammillata* embryo as in B. Detectable mitotic landmarks are indicated. Scale bar = 10 µm.